Journal of Membrane Science 492 (2015) 21–31

Contents lists available at ScienceDirect

Journal of Membrane Science

journal homepage: www.elsevier.com/locate/memsci

MOF-mixed matrix membranes: Precise dispersion of MOF particles with better compatibility via a particle fusion approach for enhanced gas separation properties

Salman Shahid [a,b,c], Kitty Nijmeijer [a], Sabrina Nehache [b], Ivo Vankelecom [c], André Deratani [b], Damien Quemener [b,*]

[a] Membrane Science & Technology, Mesa+Institute for Nanotechnology, University of Twente, P.O. Box 217, 7500 AE Enschede, The Netherlands
[b] IEM (Institut Europeen des Membranes), UMR 5635 (CNRS-ENSCM-UM2), Universite Montpellier, CC047, Place E. Bataillon, 34095 Montpellier, France
[c] Centre of Surface Chemistry and Catalysis, KU Leuven, Kasteelpark Arenberg 23-Box 2461, B-3001 Leuven, Belgium

ARTICLE INFO

Article history:
Received 14 January 2015
Received in revised form
11 April 2015
Accepted 9 May 2015
Available online 16 May 2015

Keywords:
Particle fusion
MOF
Mixed matrix membranes
High pressure
Gas separation

ABSTRACT

Mixed matrix membranes (MMMs) incorporating conventional fillers frequently suffer from insufficient adhesion between the polymer matrix and the fillers. This often results in the formation of non-selective voids at the filler/polymer interface, which decreases the performance of the membrane. A novel approach is presented here to develop metal organic framework (MOF) based MMMs by using the self-assembly of MOF and polymer particles followed by their controlled fusion. MOF-polymer interaction is optimized through this strategy and it overcomes MOF-polymer incompatibility, MOF agglomeration and MOF distribution problems, happening especially at high loadings of MOFs when applying conventional methods. Matrimid® polymer particles were first prepared by precipitating a Matrimid® polymer solution in water. The surface of these particles was then modified by the introduction of imidazole groups, enhancing the chemical compatibility with the selected ZIF-8 MOF. ZIF-8 nanoparticles were then grown in-situ to this modified polymer particle suspension by addition of the precursor for ZIF-8 synthesis. The resulted suspension was cast to dryness and annealed in a solvent–vapor environment to induce particle fusion, leading to a dense MMM structure. Scanning electron microscopy (SEM) images showed an excellent dispersion of the ZIF-8 nanoparticles forming a percolating pathway without any agglomeration, even at 40 wt% loading of the ZIF-8. Excellent dispersion of ZIF-8 and an excellent ZIF-8-polymer interfacial adhesion resulted in a significant improvement in both CO_2 permeability and CO_2/CH_4 selectivity. The CO_2 permeability of the MMMs increased by 200% and the CO_2/CH_4 selectivity increased by 65% as compared to unfilled Matrimid®. More detailed analysis of the gas transport performance of the MMMs showed that the CO_2 permeability and the CO_2/CH_4 selectivity are mainly governed by the increase in CO_2 diffusivity. The presented approach is a very versatile MMM preparation route, not only for this specific ZIF and polymer but for a wide range of material combinations.

© 2015 Elsevier B.V. All rights reserved.

1. Introduction

Membrane technology offers energy efficient and environmentally friendly separation processes and has become important for many sustainable process applications e.g. energy generation, energy storage, water purification and gas separation [1]. During the last two decades, polymeric membranes have experienced major expansion in gas separation applications and substantial research efforts have been devoted to develop new polymeric membranes to improve the membrane separation performance [2–4]. Despite all these efforts, polymeric membranes are limited by a permeability-selectivity trade-off behavior indicated via an empirical upper bound, as presented in the famous Robeson plot [5,6]. On the other hand, inorganic membrane materials offer excellent separation performances combined with high chemical and thermal stability in contrast to polymeric membranes [1]. However, the biggest hurdle in large scale production of inorganic membranes lies in their high cost and lack of processability [7]. Mixed matrix membranes (MMMs) offer the opportunity to combine the benefits of low cost and easy processing of polymeric materials with the excellent transport performance of inorganic fillers. Successful implementation of this approach can produce robust membranes with enhanced permeability and selectivity exceeding the Robeson upper bound limit [8]. However, MMMs

* Corresponding author.
E-mail address: Damien.Quemener@univ-montp2.fr (D. Quemener).

http://dx.doi.org/10.1016/j.memsci.2015.05.015
0376-7388/© 2015 Elsevier B.V. All rights reserved.

often do not operate at their predicted separation performance behavior, due to an insufficient adhesion between the polymer matrix and the fillers [9]. The polymer-filler interface morphology is a critical factor to determine the overall gas transport properties as poor interaction between the polymer and filler could lead to non-selective void formation, which results in high fluxes but low selectivities [10–13].

Recently, metal organic frameworks (MOFs) have been identified as attractive fillers. Due to the high flexibility of the MOF design, these allow to specifically tune their properties towards high selectivity and permeability for specific separations. At the same time, the current MOF chemistry allows to some extent to improve the embedding of the MOF in the polymer matrix [14]. Nevertheless, still non-selective voids at the MOF-polymer matrix interface are frequently formed [14,15].

Perez et al. [16] incorporated MOF-5 in a Matrimid® matrix for the separation of binary mixtures. At 30 wt% loading, permeability of gases increased by 120%. Nevertheless, this increase was the result of MOF aggregation and poor interconnectivity at the interface between MOF and polymer matrix, as observed by scanning electron microscopy (SEM).

In other studies, Cu-4,4′-bipyridine-hexafluorosilicate (Cu-BPY-HFS) and $Cu_3(BTC)_2$ were embedded in a Matrimid® polymer matrix [17,18]. In both studies, enhanced gas permeability was observed while the selectivity remained approximately equal to that of the unfilled polymer. Ordonez et al. [19] studied a Matrimid®-ZIF-8 MMMs. The permeability of these membranes was enhanced with increasing loading of ZIF-8 up to 40 wt%. The published SEM images showed aggregated ZIF-8 particles in the polymer matrix with visible interfacial voids.

Ploegmakers et al. [20] observed that the $Cu_3(BTC)_2$ crystals were deposited at the bottom of the membrane during the membrane preparation, leading to an inhomogeneous membrane. The resulting MMMs showed an increased selectivity with $Cu_3(BTC)_2$ loading while the permeability remained constant.

Recently, Song et al. [21] reported MMMs prepared using as-synthesized non-dried ZIF-8 nanoparticles in Matrimid®. The as-synthesized ZIF-8 particles showed a relatively better compatibility with the polymer matrix compared to previously reported ZIF-8 MMMs [19,22,23]. But still at high loadings (>20 wt%), the MMMs showed enhanced CO_2 permeability combined with decreased selectivity, even below that of the native polymer, attributed to non-selective voids.

Several attempts have been reported to improve the interaction between polymer and fillers, including proper selection of compatible polymers and filler particles [9,24], priming of filler particles [25], use of more concentrated (viscous) suspensions [26], controlling evaporation rates of solvents [27], use of silane coupling agents [28–30], annealing treatments [21] and coating the outer surface of MMMs with thin appropriate layers. But the fabrication of the MMMs poses several challenges as mentioned above in order to obtain the desired morphology, gas separation properties and mechanical/chemical stability.

To enhance the performance of polymer-MOF MMMs tremendously, we here report a novel strategy to prepare high-performing MOF-polymer MMMs by using particle fusion of polymer particles and the in-situ synthesized MOF particles.

First PI polymer particles are prepared by precipitating a Matrimid® solution into a non-solvent. Subsequently the surface of these particles is chemically modified by introduction of a MOF compatible functionality (i.e. imidazole). The MOF particles are then grown into an aqueous suspension of these modified polymer particles by addition of the MOF precursors. The resulting suspension is cast onto a flat substrate and dried in a solvent–vapor environment to transform the particulate morphology into a dense MMM structure.

Surface modification of polymer, in-situ growth of MOF particles in a polymer particle suspension and subsequent fusion of the polymer particles in a controlled solvent vapor environment offers a new, highly versatile and easy method to prepare polymer-MOF MMMs without encountering the usual problem of poor MOF-polymer adhesion between MOF and polymer as observed in MMMs prepared by standard mixing and membrane casting. Growing the MOF in the spaces between the polymer particles will provide a more continuous MOF phase throughout the membrane without agglomeration, even at higher loadings. The proposed method of particle fusion improves the MOF-polymer interactions far more than the solvent casting method and eliminates the major obstacles stemming from polymer-MOF incompatibility, MOF agglomeration and MOF misdistribution, pore blockage and chain rigidification.

ZIF-8 and Matrimid® PI are selected as model MOF and polymer matrix. The reason for choosing this particular MOF is threefold; (i) it is readily available and well understood in terms of structure and behavior, (ii) it has excellent thermal, chemical and moisture resistance and (iii) it has been widely used in CO_2/CH_4 gas separation studies. Several experimental and simulation studies based on the adsorption and separation of natural gas showed high potential of ZIF-8 as adsorbent material [31–33]. Matrimid® is a widely used PI in industry because of its high glass transition temperature and good processability. Nevertheless, the proposed particle fusion method is very versatile and can be applied to many other combinations of polymer and MOF.

In this approach, polyimide polymer particles are first prepared by emulsifying the Matrimid® polyimide polymer solution into a non-solvent. The surface of these particles is chemically modified by introducing imidazole functionality. The ZIF-8 particles are then grown into this modified polymer particles suspension by addition of the precursors for ZIF-8 synthesis. The resulted suspension is cast onto a flat substrate and dried in a controlled solvent–vapor environment to transform the particulate morphology into dense MMMs.

The characteristics of the MMMs prepared through this novel particle fusion approach are investigated by a multitude of characterization techniques e.g. XRD, FTIR, NMR, TGA, DSC etc. Additionally the effect of ZIF-8 in terms of gas separation performance of the MMMs is studied and the results confirm the exceptionally good performance of the obtained membranes. As such, the MMMs prepared by the developed particle fusion approach clearly outperform MMMs prepared by traditional polymer-MOF mixing and subsequent membrane casting.

2. Experimental

2.1. Materials

Matrimid® 5218 PI was supplied by Huntsman, Germany. The number average molecular weight was 50000 g mol^{-1} with a polydispersity of 1.62, as analyzed by gel permeation chromatography (GPC) calibrated by polystyrene standards. Zinc nitrate hexahydrate $[Zn(NO_3)_2.6H_2O]$ and 2-methylimidazole $[C_4H_6N_2]$ were obtained from Sigma-Aldrich. Mili-Q water (with a resistivity of 18.0 MΩ cm) was used for the aqueous synthesis of ZIF-8. DMF (99% extra pure) was used as a solvent for the polymer and was purchased from Acros Organics, Belgium. All solvents were of analytical grade and used without further purification. CO_2, CH_4 and a mixture of (50/50 mol% CO_2/CH_4) were supplied by Praxair, The Netherlands, and used as received (purity 99.999%).

2.2. Membrane preparation

2.2.1. Synthesis of ZIF-8 nanocrystals

The ZIF-8 nanocrystals were synthesized in either aqueous conditions at room temperature [34] or under microwave irradiation conditions [31]. For both methods starting reactants were Zn $(NO_3)_2 \cdot 6H_2O$ and 2-methylimidazole. 0.13 g of $Zn(NO_3)_2 \cdot 6H_2O$ was dissolved in 3 g Mili-Q water. Secondly, 2.5 g 2-methylimidazole was dissolved in another 6.8 g Mili-Q water. The zinc nitrate solution was then dropwise added to the 2-methylimidazole solution under stirring at room temperature. The synthesis solution turned milky almost instantly after the two solutions mixed. After stirring for 12 h, the product was collected by centrifuging and then washed with deionized water (DI) for several times. For the microwave assisted synthesis of ZIF-8, the same recipe was used as for the synthesis at room temperature. The reactants were mixed in a Teflon-lined autoclave. Synthesis was carried out at 140 °C for 2 h in a Milestone ATC-FO 300 microwave oven, equipped with a MultiSYNTH Touch Screen Controller-Terminal 640. The mixture was heated to 140 °C for 2 h using a microwave power of 300 W. The resulting powder was recovered by centrifugation and washed with DI water for several times. The yield of both syntheses was ~80% based on the amount of zinc. As model samples, two batches of ZIF-8 nanocrystals were as well dried under vacuum at 100 °C for 24 h and stored dry for further analysis.

2.2.2. Synthesis and modification of the polymer particles

A 3, 5, 8 and 10 wt% Matrimid® solution in DMF was prepared. The solutions were stirred at room temperature overnight to make sure that the Matrimid® was completely dissolved. The final solutions were left for 2–3 h to allow complete release of air bubbles. The polymer solutions were subsequently injected in the form of droplets into a water tank using a fine stainless steel syringe tip with a size of 18 G (inner diameter of 0.7 mm) at a flow rate of 1 ml/min. For the rapid breaking of the polymer droplets, a Branson digital sonifier probe (101-135-066R) was used with a 100% probe amplitude. Solid polymer spheres were formed immediately in water via solvent/water exchange. The resulting polymer spheres were dialysed to remove solvent using a cellulose dialysis tubing from Sigma-Aldrich with a MWCO value of 12000 Da.

The surface of the polymer particles was subsequently modified by giving them an imidazole functionality using 1-(3-aminopropyl)-imidazole as a linker. An amount of 1-(3-aminopropyl)-imidazole equivalent to 10 wt% of the polymer quantity was added to the suspension of the polymer particles under stirring at room temperature for 3–4 h. The chemical structure of the resulting material was confirmed by ^{1}H NMR and FTIR. The percentage of modification was evaluated by ^{1}H NMR, as explained in the supporting information.

2.2.3. Preparation of unfilled membranes and MMMs from a mixture of phase separated polymer particles and ZIF-8

To prepare the MMMs, the surface modified polymer particles (prepared from 8 wt% Matrimid® solution, as described above) were used. The ZIF-8 particles were grown into this modified polymer particle suspension by addition of the precursors (Zn $(NO_3)_2 \cdot 6H_2O$ and 2-methylimidazole) for ZIF-8 synthesis using the same procedure as used for pure ZIF-8 nanocrystals synthesis. The resulting suspension was uniformly cast on a glass plate using a casting knife [300 μm slit] and the film was kept in a controlled DMF vapor environment for 5 days to dissolve the polymer particles around the ZIF-8 particles and to obtain dense MMMs. Finally, the resulting dense MMMs were vacuum dried at 150 °C for 24 h. The same procedure was used to prepare unfilled polymer membranes without ZIF-8 particles.

2.3. Characterization techniques

Scanning electron microscopy (SEM) was performed using a low vacuum SEM (Hitachi S-4500) operated at a spatial resolution of 1.5 nm. The samples for SEM characterization were prepared by freeze-fracturing the dried membranes in liquid nitrogen. The samples were coated with a 1.5–2 nm thin platinum layer using a Balzers Union SCD040 sputter coater under argon flow to reduce sample charging under the electron beam.

The crystallinity of the samples under study was determined by powder X-ray diffraction (XRD) on a Bruker D2 PHASER operated at 40 mA and 40 kV using CuKα radiation with a wavelength (λ)= 1.54 Å at room temperature. Scans were made from 5° to 50° 2θ with a step size of 0.02° and a scan speed of 0.2 s per step. The membrane sample was attached onto a sample holder with a single crystal silicon substrate.

Thermal stability of the membranes was investigated by Thermal Gravimetric Analysis (TGA) using a Perkin-Elmer TGA 4000. Samples were heated in N_2 from 50 °C to 900 °C at a ramp of 20 °C/min. The values reported in this study are an average of 3 membranes.

The glass transition temperature (*Tg*) of the membranes was determined on a Perkin-Elmer 8000 differential scanning calorimeter. The samples were heated to a temperature of 400 °C at a temperature ramp of 10 °C/min. Then, the samples were quenched back to 50 °C at 10 °C/min. This cycle was repeated two times. The *Tg* was determined from the second heating scan using the midpoint heat capacity transition method.

^{1}H NMR (Nuclear Magnetic Resonance) spectra were recorded on a 300-MHz Bruker ACF300 spectrometer using deuterated chloroform as solvent (chloroform-d, Sigma-Aldrich, 99.9%).

The mechanical strength testing of the membranes with different ZIF-8 loadings was performed on a dynamic mechanical analyzer (DMAQ800) at a frequency of 2 Hz. Film samples with approximate dimensions of $17 \times 5 \times 0.1$ mm^3 were mounted in jaws. An average of 3 membranes was reported.

Fourier transform infrared spectroscopy (FTIR) was performed on a FTIR 710 de Nicolet over a wavelength range of 400–4000 cm^{-1}, with a spectral resolution of 4 cm^{-1} and 32 scans. Thin slices of pure and mixed matrix membranes were measured directly.

Nitrogen adsorption analysis at 77 K was conducted using a Tristar 3000 instrument. The membrane sample (0.1 g) was cut into small pieces. All samples were degassed at 150 °C overnight under a helium blanket and then placed in the adsorption station for analysis. The apparent surface area was calculated using the Brunauer–Emmett–Teller (BET) equation [35].

Gas sorption measurements of the fabricated membranes and pure ZIF-8 were performed on a Rubotherm Präzisions Mess Techniek GmBH magnetic suspension balance. Approximately 50 mg of the sample was placed in the sample holder and evacuated till constant weight was achieved (to remove all air and water vapor from the sample). In order to determine the exact weight of the sample, a measurement at 0 bar pressure was conducted. After the measurement showed a constant value, the pressure was increased by introducing either pure CO_2 or pure CH_4 into the system. The measurement was conducted at pressures of 0, 1, 2, 5 and 10 bars. The temperature was kept constant in the range of 35.0 ± 0.5 °C. The measured weight w_t (g) was corrected for buoyancy according to Archimede's principle. On the basis of the exact sample volume V_t (cm^3) and the initial weight w_0 (g) of the sample and the gas density ρ_g (g/cm^3), the mass gain m_t

(g) could be calculated:

$$m_t = \left(w_t + V_t\,\rho_g\right) - w_0 \quad (1)$$

The gas density was estimated using the Peng Robinson equation of state. The gas concentration in the polymer (cm^3 (STP) gas per cm^3 of polymer) was calculated using the molar volume at standard temperature and pressure (STP, 1 bar and 273.15 K), the polymer volume, and the molecular weight of the specific gas. The sorption isotherms were curve fitted by using a dual mode sorption model. Subsequently the solubility of the gas in the polymer (cm^3(STP)/$cm^3 \cdot$ cmHg), was calculated as:

$$S_i = \frac{C_i}{p_i} \quad (2)$$

where C_i is the gas concentration in the polymer (cm^3(STP)/cm^3), p_i is the partial pressure of component i (cmHg).

2.3.1. Gas permeation

Gas permeability measurements were performed using a constant volume-variable pressure permeation cell with vacuum at the permeate side, as described elsewhere [36]. The desired feed pressure was applied at the top side of the membrane while keeping the permeate side under vacuum. The gas permeability values were calculated from the increase in pressure in a calibrated volume. A mixture of CO_2 and CH_4 (50/50 mol%) was used to investigate the membrane performance. All membranes were vacuumed overnight prior to testing. In all cases, two to three samples from different membranes of the same composition were measured. The samples were measured continuously at a temperature of 35 °C and a retentate flow of 5 cm^3/min. Furthermore, in order to exclude time effects, permeability values were taken after 8 h of measurement. The gas that permeated through the membrane was collected and directly injected into a Varian 3900 GC gas chromatograph using an Alltech alumina F-1 60/80 packed bed column at 150 °C to analyze the composition of the permeate.

3. Results and discussion

The synthesized ZIF-8 nanoparticles were characterized by various characterization techniques. The morphological features of the nanocrystals are of great importance for the preparation of MMMs, as these influence the distribution of the filler particles in the polymer matrix and the interactions at the interface between filler and polymer. As revealed by SEM (Fig. 1), the synthesized ZIF-8 consisted of homogeneous dodecahedron crystals. The average crystal dimensions were ca. 120 nm after aqueous synthesis and slightly smaller crystals were obtained by microwave heating (95 nm). The use of the (fast) microwave heating method has been reported to reduce the synthesis time and to result in smaller and more uniformly sized MOF crystals compared to the aqueous room temperature synthesis method [31].

Fig. S1 (Supporting information)) shows the XRD patterns for the synthesized ZIF-8 materials. Virtually identical diffractograms were observed for all ZIF-8 samples, irrespective the synthesis method. This pattern is in agreement with the literature [21], indicating that pure ZIF-8 indeed was obtained.

In line with the XRD results, N_2 adsorption did not indicate any significant differences in the porous structure of ZIF-8 for the two synthesis methods (Fig. S2). BET surface areas of respectively 1300 m^2/g and 1450 m^2/g were obtained for the aqueous room temperature and microwave assisted synthesized ZIF-8 nanocrystals.

In summary, physico–chemical characterization of the synthesized ZIF-8 nanocrystals evidenced that the heating method applied during the synthesis does not have a significant influence on the properties of the final product in the case of ZIF-8. Based on these results and its ease of synthesis, the aqueous synthesis of ZIF-8 at room temperature was selected to be used in the assembly of the MMMs. All later discussion on MMMs contained ZIF-8 nanocrystals synthesized at room temperature in aqueous conditions.

3.1. Synthesis of polymer particles: effect of polymer solution concentration

Fig. 2 shows the SEM images of the polymer particles prepared from different concentrations of polymer solutions. The size of the polymer particles increases when the polymer concentration increases. A 3 wt% polymer solution generated polymer particles of ca. 20–30 nm, while an 8 wt% polymer solution resulted in ca. 40–50 nm particles. At polymer concentrations higher than 10 wt %, clumps of polymer beads (1–2 μm) were observed instead of individual nanoparticles. The dependence of the particle size on the polymer concentration, stirring speed and precipitation temperature is well known [37]. An increase in the polymer content will increase the solution viscosity and the fragmentation stage of the emulsification process will be altered. As membranes prepared from solutions with polymer concentrations below 8 wt% experienced higher shrinkage leading to cracks in the final membrane, the 8 wt% polymer solution was selected for membranes preparation.

3.2. Polymer modification via grafting of 1-(3-aminopropyl)-imidazole

The grafting of 1-(3-aminopropyl)-imidazole on Matrimid® beads was done via an imide ring opening reaction induced by 1-(3-aminopropyl)-imidazole. As shown in Scheme 1, the amine group of 1-(3-aminopropyl)-imidazole reacts with the imide functions in Matrimid® to form ortho-diamide functions. The chemical structures of the resulting 'polyimide-amide' materials

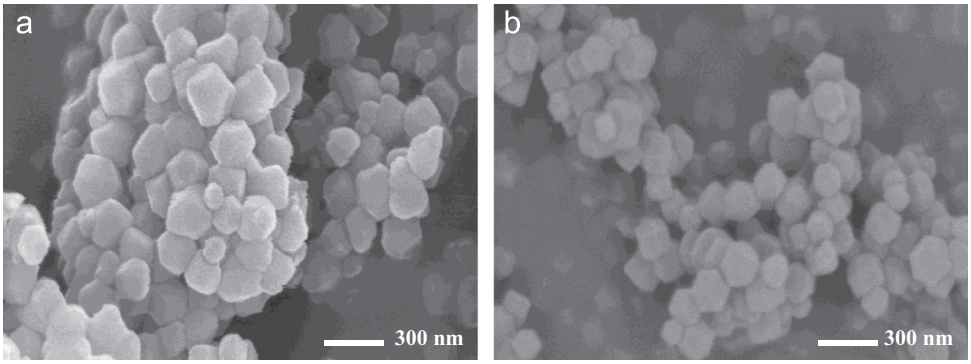

Fig. 1. SEM images of ZIF-8 nanoparticles prepared by (a) aqueous room temperature method and (b) microwave assisted method. (Magnification: (a) and (b): 100,000 ×).

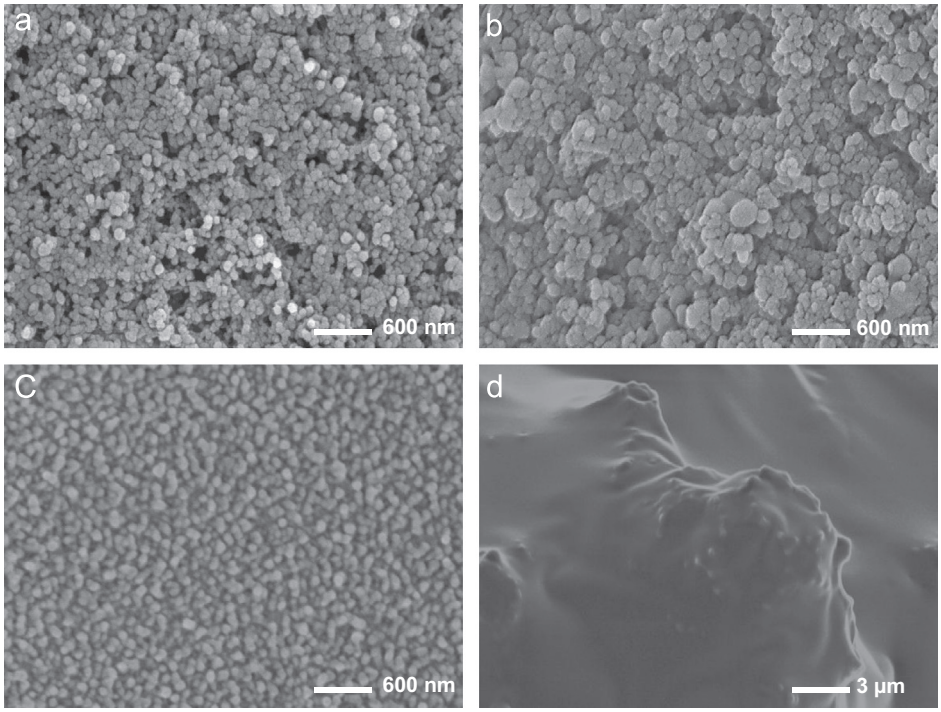

Fig. 2. SEM images of polymer particles prepared from polymer solutions containing different polymer concentrations (Magnification: (a)–(c): 50,000 × and (d): 10,000 ×).

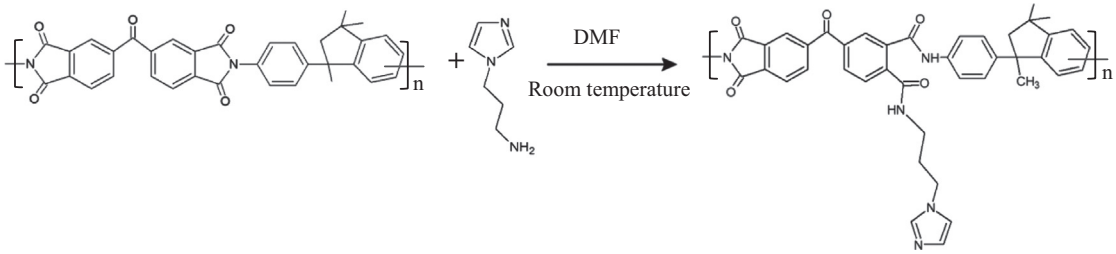

Scheme 1. Grafting of 1-(3-aminopropyl)-imidazole on Matrimid®.

(referred to as modified Matrimid® from now on) were confirmed by ^{1}H NMR (Figs. S3 and S4 (Supporting information)) and FTIR (Fig. S5). The percentage of modification was evaluated by ^{1}H NMR. Details of the calculation of the modification degree are given in the supporting information.

As known from literature, the modification of the particle surface chemistry can facilitate the assembly of the particles (Fig. S6) [38]. In a synergistic effect, the amine modification of Matrimid® will also result in improved CO_2 gas permeabilities [39], while the pendent imidazole units will lead to a better compatibility between the polymer phase and the ZIF-8 nanoparticles.

3.3. Characterization of MMMs

To prepare MMMs, ZIF-8 nanocrystals were grown in the spaces between the polymer particles. Fig. S7 shows SEM images of mixtures of polymer particles at different ZIF-8 loadings. In all cases the ZIF-8 nanoparticles are homogeneously dispersed among the polymer particles and no agglomeration of ZIF-8 nanoparticles is observed, even at high loadings (30 wt% and 40 wt%). In a trial experiment simple mixing by sonification of polymer beads and ZIF-8 particles was also investigated to compare this with in-situ growth of ZIF-8. The mixing of particles led to poor dispersion of ZIF-8. Fig. S8 shows the SEM images of mixtures of polymer and ZIF-8 particles prepared through simple mixing. The relatively poor dispersion and separate polymer and ZIF-8 particle domains are quite visible. The adhesion between polymer and ZIF-particles is bad. Thus, for excellent dispersion of ZIF-8 nanoparticles, in-situ growth of ZIF-8 nanoparticles was selected and all the later discussion involves MMMs prepared via in-situ growth of ZIF-8 nanoparticles.

In order to obtain a dense MMM structure, suspensions of polymer particles with different ZIF-8 loadings were cast, dried and subsequently exposed to a saturated atmosphere of DMF vapors at room temperature for 5 days. Fig. 3 shows the surface and cross-sectional SEM images of the transformation of the particulate morphology into a dense MMMs morphology over a total period of 5 days.

While water evaporation leads to the formation of a solid film through the assembly of particles, the exposure to DMF vapor leads to a controlled fusion of the polymer particles into a dense layer, progressing from the top to the bottom of the membrane with progressing annealing time (Fig. 3). In the cross-section, it is visible that this densification starts from the top, as the solvent starts to sorb at the top surface, and slowly moves towards the lower parts of the cross-section. During transformation from a particle morphology to a dense MMM structure, the color also changes from slightly opaque yellowish to a translucent amber.

SEM images of the cross-section of a 30 wt% MMM are shown in Fig. 4. For comparison, a 30 wt% MMM was prepared using dried ZIF-8 nanoparticles (conventional solution casting approach) is also shown. This membrane shows aggregation of ZIF-8 particles

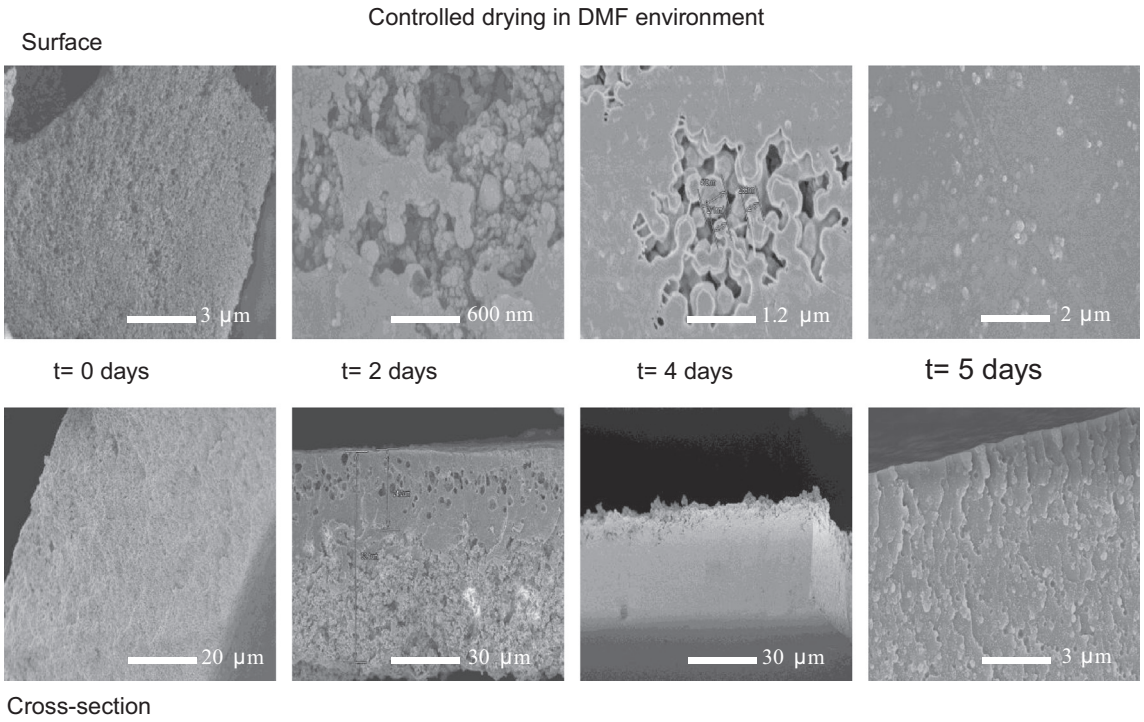

Fig. 3. Surface and cross-sectional transformation from particulate morphology to dense MMM morphology over a period of 5 days. Specific solvent vapor annealing time (t) is also shown in Fig. 3.

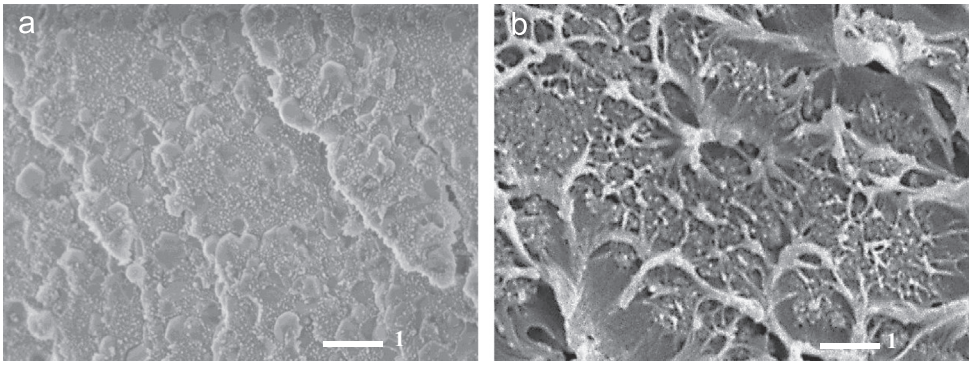

Fig. 4. MMM containing 30 wt% ZIF-8 prepared by (a) particle fusion and (b) conventional solution casting. (Magnification: (a): 25,000 × and (b): 20,000 ×).

and poor adhesion at the ZIF-8 polymer interface. Also the ZIF-8 particles show poor dispersion in some regions of the cross-section. On the contrary, MMMs prepared by particle fusion show ZIF-8 nanocrystals completely wrapped by the polymer matrix. Fracturing under liquid N_2 causes the polymer layer to break without plastic deformation, giving a more smooth cross-section than the crater-like morphology obtained for conventional solution cast membranes [40]. Using the particle fusion approach, excellent dispersion of ZIF-8 nanoparticles in the polymer matrix (up to ZIF-8 loadings of 40 wt%), were obtained. Large aggregates of ZIF-8 particles are not observed. Each ZIF-8 particle is separated by a very thin layer of the matrix polymer theoretically creating an ideal percolating pathway for gas permeation. At higher loadings (40 wt%), the MMMs do show good dispersion and good contact between the ZIF-8 nanoparticles and the polymer, but the membranes are very brittle in terms of mechanical properties. The particle fusion technique significantly improved the particle dispersion and interface morphology as compared to previous work on such MMM systems [19,21,23,41,42].

XRD patterns of the unfilled polymer and the mixed matrix membranes are presented in Fig. S9. The unfilled Matrimid® polymer membrane is completely amorphous and shows a broad spectrum, typical for amorphous materials. For all the Matrimid®-ZIF-8 MMMs, the crystalline structure of the ZIF-8 nanoparticles is clearly the same as that of pure ZIF-8.

The thermal stability of the synthesized ZIF-8, as evaluated by TGA is presented in Fig. S10. Fig. S10 shows no significant weight loss till 200 °C due to the hydrophobic pores of ZIF-8 that prevents adsorption of e.g. water vapor [43]. At temperature above 450 °C degradation of ZIF-8 occurs, which is in agreement with literature [44]. By comparison, the thermal degradation of modified Matrimid® starts around 485 °C and increases with increasing MOF content up to 500 °C for MMMs with up to 30 wt% ZIF-8. The increase in thermal stability of the MMMs can be attributed to the high thermal stability of the ZIF-8 nanoparticles and the existence of favorable interactions between the ZIF-8 and the modified Matrimid® polymer matrix.

Table 1 shows the glass transition temperature of the different membranes measured by DSC. The glass transition temperature of unfilled Matrimid® (unmodified) is 328 °C, which is consistent with literature [45]. The surface modified pure Matrimid® shows a Tg around 278 °C. This drop in Tg can be attributed to plasticization caused by the surface modifier (the molecular weight

Table 1
Glass transition temperature and mechanical properties of MMMs with different ZIF-8 loadings.

Polymer content (wt%)	MOF loading (wt%)	*Tg* (°C)[a]	Young's modulus (GPa)	Tensile strength (MPa)	Elongation at break (%)
100 (non-modified)	0	328	2.5	107	119
100 (modified)	0	278	2.35	111	125
90	10	282	2.91	98	104
80	20	289	3.42	93	95
70	30	295	3.63	85	85
60	40	300	3.51	80	70

[a] Typical error in DSC results ranges from ± 1–1.5 °C.

measurement did not show a reduction in molecular weight as confirmed by GPC (not shown here)). The 1-(3-aminopropyl)-imidazole linker increases the inter-chain distance, giving the polymer chains more inter-segmental mobility. Moreover, the rigid imide ring is opened upon reaction. The decrease in *Tg* provides additional conformational flexibility and better contact between filler and polymer. Hence less brittle membranes are obtained.

For MMMs, the *Tg* increases from 278 °C to 300 °C with increasing ZIF-8 loading. At low ZIF-8 loadings, the increase in *Tg* is low, but at loadings of 40 wt%, a significant increase of 22 °C in the *Tg* is observed (Table 1), indicating a restricted chain movement. As mentioned before, each ZIF-8 nanoparticle is surrounded by a thin layer of the polymer, significantly restricting the polymer chain movement. Additionally, the strong polymer–particle interactions, thanks to the particle surface modification, increase the *Tg*. Such phenomenon has also been observed for Cu-BPY-HFS/Matrimid® [18]. Chung et al. prepared Matrimid® membranes containing benzylamine-modified C_{60} and a 14 °C increase in *Tg* was reported, which indicates a strong interfacial interaction between Matrimid® and the benzylamine-modified C_{60} particles [45].

The influence of the ZIF-8 content on the Young's modulus is shown in Table 1. The Young's modulus of the MMMs exhibits a linear increase with increasing ZIF-8 loading up to 30 wt%, followed by a decrease at 40 wt% ZIF-8 loading. The increase in Young's modulus suggests that the interfacial adhesion between the ZIF-8 nanoparticles and the polymer chains is good [46] up to 30 wt% loading of ZIF-8. This is higher than that of other reported ZIF-8-MMMs systems [19,44]. This enhanced compatibility between ZIF-8 and the polymer chains can be attributed to the imidazolate functionality of the polymer and ZIF-8. However, at a loading of 40 wt%, the MMM becomes more brittle, resulting in a decreased Young's modulus. This effect might be due to the slight aggregation of the ZIF-8 nanoparticles at higher loadings, resulting in less contact between the ZIF-8 nanoparticles and the polymer matrix. Both the tensile strength and the elongation at break decrease with increasing ZIF-8 loading due to the reduced flexibility caused by the presence of ZIF-8 nanoparticles [47] and the formation of a more rigid MMM with increasing ZIF-8 loading [18]. Such phenomenon has also been observed for other MOF/Matrimid® systems [44].

3.4. Gas separation

3.4.1. Gas sorption

Both CO_2 and CH_4 show a dual mode sorption isotherm in the different membranes as shown in Figs. S12 and S13. The results are quite consistant with literature [21]. Fitting the data with the dual mode sorption model provides the parameters summarized in Table 2.

CO_2 shows a higher sorption compared to CH_4, attributed to the higher critical temperature (T_c) and consequently enhanced condensability of CO_2 compared to CH_4 (T_c-CO_2: 304 K, T_c-CH_4: 190 K) [1]. Also the favorable quadrupolar interactions of CO_2 contribute to this. In comparison to the unfilled polymer membranes, pure ZIF-8 shows a higher adsorption attributed to the high surface area of the nanoparticles. The crystallographic pore aperture of ZIF-8 crystals is 3.4 Å, ideally, it would only allow the transport of gas molecules with smaller kinetic diameter blocking the large molecules including CH_4 (3.8 Å). However, an increase in CH_4 sorption was also observed that can be attributed to the structural flexibility of ZIF-8 [48]. The results tabulated in Table 2 for the MMMs suggest that the addition of ZIF-8 in the Matrimid® membrane affects both the Langmuir and the Henry's sorption. Compared to unfilled Matrimid® membranes, the value of k_D decreases as the ZIF-8 loading increases, indicating that overall sorption is dominated by Langmuir sorption (in the nanocages of ZIF-8) at higher filler loadings. The presence of ZIF-8 particles in the MMMs provides extra sorption sites for both gases (more for CO_2 than for CH_4) that lead to higher C'_H and *b* values for both CO_2 and CH_4 with increasing ZIF-8 loading. The increasing values of $C_{H'}$ and *b* indicates the higher sorption of both gases. It was reported [49], that, at low pressures, both CO_2 and CH_4 are preferentially sorbed in the vicinity of the organic imidazolate linkers in the windows region. At high pressures, CH_4 resides near the aperture, but CO_2 sorbs in the central cage. As the pressure increases, the nanocages of ZIF-8 get saturated, leaving only Henry sorption in the polymer matrix.

Table 2
Dual mode sorption parameters for CO_2 and CH_4 in the different membranes.

Feed gas	ZIF-8	Dual mode sorption model		
	(wt%)	C'_H cm³(STP)/cm³	b (1/cmHg)	k_D (cm³(STP)/cm³ · cmHg)
CO_2	0	29.59	0.16	0.78
	0-M[a]	31.11	0.17	0.78
	10	39.28	0.17	0.69
	20	47.21	0.20	0.59
	30	57.16	0.24	0.52
	40	69.26	0.24	0.35
	100	280.20	0.26	0
CH_4	0	10.25	0.059	0.17
	0-M[a]	11.15	0.056	0.17
	10	13.10	0.057	0.14
	20	15.40	0.062	0.13
	30	16.24	0.075	0.09
	40	18.95	0.079	0.09
	100	122.0	0.102	0

[a] 0-M modified Matrimid®.

Notably the maximum sorption capacity, C'_H, in the 30 wt% MMMs decreases by a factor 5 and 8 for CO_2 and CH_4, respectively, compared to the sorption in pure ZIF-8. This difference in sorption capacity between MMMs and pure ZIF-8 can be related to the limited sorption capacity of the polymer matrix surrounding the ZIF-8 particles. This finding provides indirect evidence that the ZIF-8 nanoparticles have excellent adhesion to the polymer matrix with minimal defects at the interfaces (which would give high sorption capacities). Addition of ZIF-8 nanoparticles to the Matrimid® membranes appears to increase the maximum sorption capacity by a factor 2–3, while the ideal CO_2/CH_4 sorption selectivity is not significantly increased. Also, addition of ZIF-8 nanoparticles might have an influence on the diffusion coefficient, which will be discussed in the next sections.

3.4.2. Effect of ZIF-8 loading on gas separation performance

Fig. 5 shows the mixed gas transport data of unfilled Matrimid® membranes and MMMs with various loadings of ZIF-8. The unfilled modified Matrimid® membranes show a higher CO_2 permeability than the non-modified Matrimid® membranes. This can be

attributed to the interaction between CO_2 and the imidazolate linker of the modified polymer chains. The permeability of CH_4 remained stable. Upon addition of ZIF-8 to the MMMs, the CO_2 permeability clearly increases, while the effect on the CH_4 permeability is only very strong at a ZIF-8 loading as high as 40 wt%. Consequently, the CO_2/CH_4 selectivity significantly increases with increasing ZIF-8 loading up to 30 wt%. Modification of Matrimid® clearly improves the compatibility between ZIF-8 and the polymer matrix and consequently increases the CO_2/CH_4 selectivity of the membrane. Looking at the relative increase in permeability, this increase is definitely more dominant for CO_2 than for CH_4 (Fig. S11). The porous MOF particles provide a percolating porous network [16] that facilitate the transport of gases. Additionally, CO_2 molecules have a strong quadrupolar moment that interacts well with ZIF-8 [50]. Hence, CO_2 permeability increases considerably with increasing ZIF-8 loadings in the MMMs. This result also suggests that the 30 wt% MMM is defect-free and that the contact between the ZIF-8 nanoparticles and the polymer is excellent. At higher loadings (40 wt %), the permeability increased more than 4 times compared to that of the unfilled polymer, while the selectivity decreased, even though still maintaining a higher value (15%) than that of unfilled modified Matrimid®. This decrease could be the consequence of the presence of some minor defects (non-selective voids) at this 40 wt% loading.

Similar results were also observed by other researchers. Bae et al. [51] observed enhanced permeability and selectivity when ZIF-90 nanocrystals were incorporated into a 6FDA-DAM polymer. They estimated that the CO_2 permeability and CO_2/CH_4 selectivity of ZIF-90 was 8000 Barrer and 250, respectively. These permeation data was quite different from the data of a pure ZIF-90 membrane (1192 Barrer, selectivity of 2.8) as reported by Huang et al. [52].

Recently, Yang et al. [53] reported that addition of ZIF-7 nanoparticles to a polybenzimidazole (PBI) matrix enhanced the permeability of H_2 and selectivity over CO_2, which was also higher than that predicted from pure ZIF-7 data. They attributed the increase in selectivity to the interaction of ZIF-7 with PBI. From above discussion it can be concluded that MOF-MMMs shows different permeation behaviors compared to pure MOF membranes.

The gas sorption and separation data were further analyzed and using the solution diffusion model ($P=D\cdot S$), the corresponding diffusivities were calculated using the pure gas sorption and permeation data. As sorption data were obtained from a system with pure gas surrounding the complete sample, while

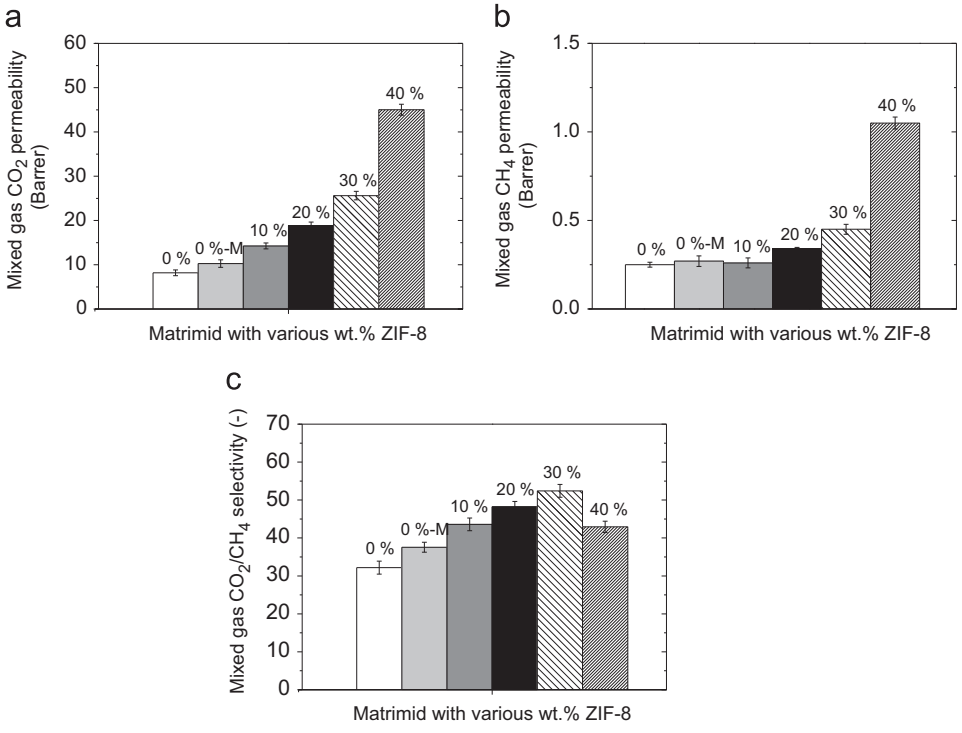

Fig. 5. Mixed gas (a) CO_2 permeability, (b) CH_4 permeability and (c) CO_2/CH_4 selectivity of prepared membranes for different ZIF-8 loadings at 5 bar and 35 °C.

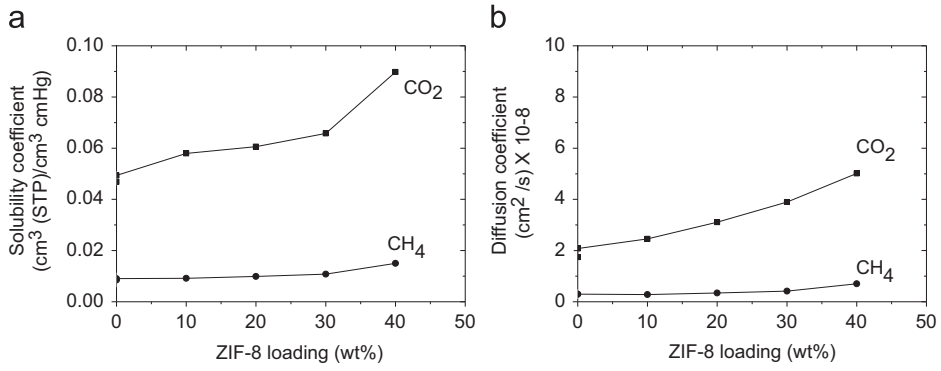

Fig. 6. Solubility and diffusion coefficients of CO_2 and CH_4 as a function of ZIF-8 loading.

permeation data were obtained from a system with mixed gas at the feed, but vacuum at the permeate side of the membrane, the diffusion data should be considered as a rough estimate only.

Fig. 6 presents the solubility and diffusion coefficients of CO_2 and CH_4 as a function of ZIF-8 loading. The solubility coefficient of both CO_2 and CH_4 increase with increasing ZIF-8 loading (Fig. 6a), althogh the increase is higher for CO_2. This leads to a slight increase in solubility selectivity at higher ZIF-8 loadings. At 40 wt% ZIF-8 loading the solubility coefficients show a swift increase that can be attributed to the presence of interfacial defects that will expose the ZIF-8 surface for adsorption. On the other hand the diffusion coefficient of CO_2 shows relatively higher increase with ZIF-8 loading compared to CH_4 (Fig. 6b). As mentioned previously, CO_2 preferentially resides in the window pore region of ZIF-8. It was reported that the preponderance of CO_2 at the window pore regions hinders the inter-cage hoping of CH_4 molecules present in the mixture with CO_2 [54]. Zhang et al. [48] also reported that for the separation a of mixture of CO_2/CH_4, the diffusion of CH_4 is distinctively hindered by the presence of CO_2 molecules in the mixture. The authors attributed this effect to the blocking of the diffusional pathway by CO_2. This blocking of CH_4 molecules by CO_2 causes the diffusion selectivity to increase. The dominant effect of diffusivity selectivity was also observed by Ploegmakers et al. for the separation of ethylene/ethane using Cu_3BTC_2 MMMs [20]. Also Thompson et al. observed an increase in diffusion selectivity of ZIF-8 MMMs for CO_2 separation from natural gas [55].

Fig. 7 presents the measured normalized solubility and diffusion coefficients of CO_2 and CH_4, as a function of the ZIF-8 loading. The data were normalized based on the data of unfilled modified Matrimid® (the absolute values of solubility and diffusion selectivities are shown in the supporting information, Fig. S14). The normalized CO_2 diffusivity increased more than the normalized diffusivity of CH_4 up to 30 wt%, but the normalized solubility of CO_2 was comparable to that of CH_4. The CH_4 diffusion coefficient showed a rapid increase in value as the ZIF-8 loading increased above 30 wt%, attributed to non-selective voids. However at all ZIF-8 loadings, the increase in normalized diffusivity was always more significant compared to the increase in normalized solubility. In ZIF-8, CO_2 has a lower energy barrier for diffusion than CH_4 and hence higher diffusivity [48]. The results show that the major contribution to the increase in mixture selectivity comes from the diffusion selectivity.

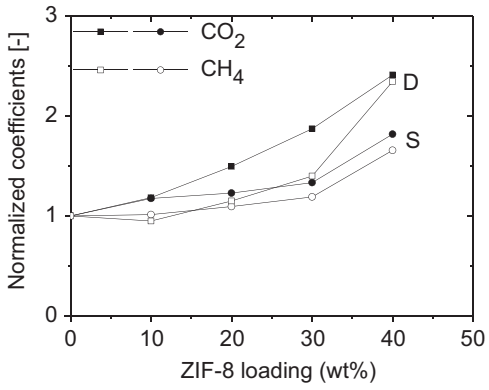

Fig. 7. Normalized solubility and diffusion coefficients for CO_2 (closed symbols) and CH_4(open symbols) as a function of ZIF-8 loading. Results are normalized based on the data of unfilled modified Matrimid®.

3.5. Overall membrane performance

A comparative study of the performance of the presented membranes with literature data for polyimide-based filled and unfilled membranes with respect to permeability and CO_2/CH_4 selectivity is shown in Fig. 7. Also other MOF-MMMs from literature are added for comparison. Table 3 presents the details and operating conditions of the data presented in Fig. 7. Due to the lack of mixed gas data available for most other MOF based MMMs systems, pure gas data for MOF based membranes from literature were also included for comparison.

The performance of the membranes developed by particle fusion was clearly better than that of the previously reported data for MMMs with identical (ZIF-8) or different MOFs as fillers (Fig. 7). Compared to other MOF-MMMs, our membranes showed much higher increase in permeability and selectivity. A systematic trend of increasing permeability and selectivity was clearly visible with increase in ZIF-8 loading. Most other literature on MOF based membranes showed either similar or lower selectivities than unfilled PI, indicating a poor interfacial contact between MOF

Table 3
Experimental details of the data presented in Fig. 7.

Code	Membrane (% of MOF)	Gas type	Casting solvent	T (°C)	P (bar)	Reference
1	PI-ZIF-8 (30)	Mix gas	DMF	35	5	This work
2	PI	Pure gas	$CHCl_3$	35	2	[18]
3	PI-ZIF-8 (30)	Mix gas	Dioxane, NMP	35	5	[40]
4	PI-MOF-5 (30)	Pure gas	$CHCl_3$	50	7	[57]
5	PI-Cu_3BTC_2 (30)	Pure gas	$CHCl_3$	50	7	[57]
6	PI-MOF-5 (30)	Pure gas	$CHCl_3$	35	4	[16]
7	PI-CuMOF (30)	Pure gas	$CHCl_3$	35	2	[18]
8	PI-ZIF-8 (30)	Pure gas	$CHCl_3$	35	3	[19]
9	PI-ZIF-8 (30)	Pure gas	$CHCl_3$	25	4	[21]
10	PI-ZIF-8-ambz (25)	Pure gas	$CHCl_3$	35	3.5	[55]
11	PI-ZIF-8 (30)	Pure gas	$CHCl_3$	35	3.5	[55]
12	PI-Cu_3BTC_2 (30)	Mix gas	Dioxane, NMP	35	5	[40]
13	PI-Fe(BTC) (30)	Mix gas	Dioxane, NMP	35	5	[36]
14	PI-ZIF-8 (30)	Mix gas	CH_2Cl_2	35	5	[44]
15	PI-MIL-53(Al) (30)	Mix gas	Dioxane, NMP	35	5	[40]
16	Crosslinked 6FDA-Durene-ZIF-8 (33)	Pure gas	$CHCl_3$	35	3.5	[58]
17	Ultem-MIL-53(Al) (15)	Mix gas	$ChCl_3$	35	10	[56]
18	PSF-Cu_3BTC_2 (10)	Pure gas	$CHCl_3$	35	–	[12]
19	6FDA-ODA-UiO-66 (25)	Mix gas	$CHCl_3$	35	10	[59]

Abbreviations: PI: Matrimid® 5218; 6FDA: 4,4_-(hexafluoroisopropylidene) diphthalic anhydride; Durene: 2,3,5,6-tetramethyl-1,4-phenylenediamine; Ultem: polyetherimide; PSF: polysulfone; ODA: 4,4′6oxydianiline; MOF-5: Zn_4O(1,4-benzene-dicarboxylate)$_3$; CuMOF (Cu-BPY-HFS): copper hexafluorosilicate (HFS) and 4, 4′-bipyridine (BPY); $CuBTC_2$: Cu-benzene-1,3,5-tricarboxylate (BTC); Fe(BTC): Fe-benzene-1,3,5-tricarboxylate; MIL-53(Al): aluminum terephthalate; ambz: 2-amino-benzimidazole; UiO-66 (Zr-BPDC): (BPDC = biphenyl-4,4′-dicarboxylate).

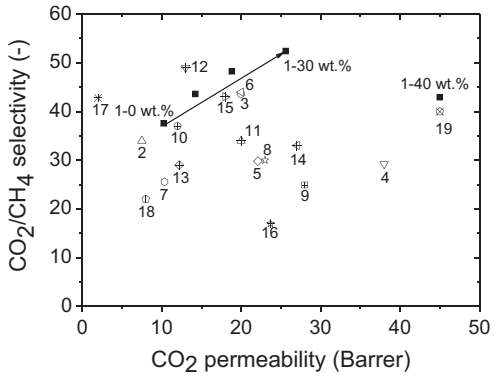

Fig. 8. Comparison study of MOF-MMMs from literature and MMMs prepared via particle fusion (this work) for CO_2/CH_4 gas separation. See Table 3 for details of different membranes and specific experimental details.

and matrix [12,19,21,51]. Particle fusion MOF based membranes showed a 200% increase in permeability combined with a 65% increase in selectivity compared to unfilled Matrimid® membranes. This indicated that it is possible to achieve much higher gas separation performances by establishing good adhesion at the interface between MOF and polymer using the particle fusion technique. It is important for future research to focus especially on highly permeable polymers e.g. 6FDA-DAM and PIM (polymers with intrinsic microporosity). Using a similar method of dispersing the MOF nanoparticles established in this study, to form defect-free MOF-MMMs, could lead to high performance membranes needed for industrial applications Fig. 8.

4. Conclusion

A facile and versatile novel route is presented for the preparation of MMMs composed of phase separated polymer particles and in-situ synthesized ZIF-8 nanoparticles with excellent adhesion between the filler and the polymer matrix. Chemical modification of the polymer led to an excellent ZIF-8-polymer interfacial compatibility. The particulate morphology of a mixture of polymer and filler particles was transformed to a dense membrane structure by DMF vapor annealing. It was possible to successfully prepare MMMs with MOF loadings as high as 30 wt% without any defects. Upon increasing the ZIF-8 loading, MMMs showed significantly better performance in the separation of CO_2/CH_4 mixtures as compared to the native polymer.The CO_2 permeability increased up to 200% combined with a 65% increase in CO_2/CH_4 selectivity, compared to the native Matrimid®. In-depth analysis of gas transport performance of the membranes showed that the higher diffusion and moderate sorption of CO_2 gas enhances the CO_2 permeability. Gas sorption studies further confirmed that the selective gas transport (CO_2/CH_4 selectivity) is mainly governed by the increase in diffusivity selectivity, which is in all cases higher than the solubility selectivity.

The overall results of our experiments show that this novel method to prepare MMMs with embedded MOF particles provides new opportunities to develop highly compatible, well dispersed and highly loaded MMMs, with enhanced permeability by proper selection of polymer matrix and high performing fillers. The approach is very versatile and can be expanded to numerous combinations of polymers and MOFs. Future work in this area will focus on the use of highly permeable polymers and more selective MOFs to prepare industrially attractive membranes.

Acknowledgements

S. Shahid acknowledges the European Commission - Education, Audiovisual and Culture Executive Agency (EACEA), for his PhD scholarship under the program: Erasmus Mundus Doctorate in Membrane Engineering – EUDIME (FPA N° 2011-0014, Edition I, http:/eudime.unical.it). D. Quemener and S. Nehache acknowledge the financial support from the "Agence Nationale pour la Recherche" (ANR-13-JS08-0008-01).

Appendix A. Supporting information

Supplementary data associated with this article can be found in the online version at http://dx.doi.org/10.1016/j.memsci.2015.05.015.

References

[1] N.N. Li, A.G. Fane, W.S.W. Ho, T. Matsuura (Eds.), Frontmatter in Advanced Membrane Technology and Applications, John Wiley & Sons, Inc., Hoboken, NJ, USA, 2008.
[2] W.J. Koros, G.K. Fleming, Membrane-based gas separation, J. Membr. Sci. 83 (1993) 1–80.
[3] R.W. Baker, Future directions of membrane gas separation technology, Ind. Eng. Chem. Res. 41 (2002) 1393–1411.
[4] P. Bernardo, E. Drioli, G. Golemme, Membrane gas separation: a review/state of the art, Ind. Eng. Chem. Res. 48 (2009) 4638–4663.
[5] L.M. Robeson, Correlation of separation factor versus permeability for polymeric membranes, J. Membr. Sci. 62 (1991) 165–185.
[6] L.M. Robeson, The upper bound revisited, J. Membr. Sci. 320 (2008) 390–400.
[7] Y. Zhang, J. Sunarso, S. Liu, R. Wang, Current status and development of membranes for CO2/CH4 separation: a review, Int. J. Greenhouse Gas Control 12 (2013) 84–107.
[8] T.S. Chung, L.Y. Jiang, Y. Li, S. Kulprathipanja, Mixed matrix membranes (MMMs) comprising organic polymers with dispersed inorganic fillers for gas separation, Prog. Polym. Sci. 32 (2007) 483–507.
[9] G. Dong, H. Li, V. Chen, Challenges and opportunities for mixed-matrix membranes for gas separation, J. Mater. Chem. A 1 (2013) 4610–4630.
[10] J.T. Chen, C.C. Shih, Y.J. Fu, S.H. Huang, C.C. Hu, K.R. Lee, J.Y. Lai, Zeolite-filled porous mixed matrix membranes for air separation, Ind. Eng. Chem. Res. 53 (2014) 2781–2789.
[11] F. Dorosti, M.R. Omidkhah, M.Z. Pedram, F. Moghadam, Fabrication and characterization of polysulfone/polyimide-zeolite mixed matrix membrane for gas separation, Chem. Eng. J. 171 (2011) 1469–1476.
[12] A. Car, C. Stropnik, K.-V. Peinemann, Hybrid membrane materials with different metal–organic frameworks (MOFs) for gas separation, Desalination 200 (2006) 424–426.
[13] S. Husain, W.J. Koros, Mixed matrix hollow fiber membranes made with modified HSSZ-13 zeolite in polyetherimide polymer matrix for gas separation, J. Membr. Sci. 288 (2007) 195–207.
[14] H.B.T. Jeazet, C. Staudt, C. Janiak, Metal–organic frameworks in mixed-matrix membranes for gas separation, Dalton Trans. 41 (2012) 14003–14027.
[15] T.T. Moore, W.J. Koros, Non-ideal effects in organic–inorganic materials for gas separation membranes, J. Mol. Struct. 739 (2005) 87–98.
[16] E.V. Perez, K.J. Balkus Jr., J.P. Ferraris, I.H. Musselman, Mixed-matrix membranes containing MOF-5 for gas separations, J. Membr. Sci. 328 (2009) 165–173.
[17] S. Basu, A. Cano-Odena, I.F.J. Vankelecom, Asymmetric Matrimid (R)/Cu-3(BTC) (2) mixed-matrix membranes for gas separations, J. Membr. Sci. 362 (2010) 478–487.
[18] Y. Zhang, I.H. Musseman, J.P. Ferraris, K.J. Balkus Jr., Gas permeability properties of Matrimid (R) membranes containing the metal–organic framework Cu-BPY-HFS, J. Membr. Sci. 313 (2008) 170–181.
[19] M.J.C. Ordonez, K.J. Balkus, J.P. Ferraris, I.H. Musselman, Molecular sieving realized with ZIF-8/Matrimid (R) mixed-matrix membranes, J. Membr. Sci. 361 (2010) 28–37.
[20] J. Ploegmakers, S. Japip, K. Nijmeijer, Mixed matrix membranes containing MOFs for ethylene/ethane separation-Part B: Effect of Cu3BTC2 on membrane transport properties, J. Membr. Sci. 428 (2013) 331–340.
[21] Q. Song, S.K. Nataraj, M.V. Roussenova, J.C. Tan, D.J. Hughes, W. Li, P. Bourgoin, M.A. Alam, A.K. Cheetham, S.A. Al-Muhtaseb, E. Sivaniah, Zeolitic imidazolate framework (ZIF-8) based polymer nanocomposite membranes for gas separation, Energy Environ. Sci. 5 (2012) 8359–8369.
[22] C. Zhang, Y. Dai, J.R. Johnson, O. Karvan, W.J. Koros, High performance ZIF-8/6FDA-DAM mixed matrix membrane for propylene/propane separations, J. Membr. Sci. 389 (2012) 34–42.
[23] Y. Dai, J.R. Johnson, O. Karvan, D.S. Sholl, W.J. Koros, Ultem((R))/ZIF-8 mixed matrix hollow fiber membranes for CO2/N-2 separations, J. Membr. Sci. 401 (2012) 76–82.

[24] R.W. Baker, Future directions of membrane gas separation technology, Ind. Eng. Chem. Res. 41 (2002) 1393–1411.
[25] R. Mahajan, W.J. Koros, Mixed matrix membrane materials with glassy polymers. Part 1, Polym. Eng. Sci. 42 (2002) 1420–1431.
[26] R. Mahajan, W.J. Koros, Factors controlling successful formation of mixed-matrix gas separation materials, Ind. Eng. Chem. Res. 39 (2000) 2692–2696.
[27] T. Rodenas, M. van Dalen, E. García-Pérez, P. Serra-Crespo, B. Zornoza, F. Kapteijn, J. Gascon, Visualizing MOF mixed matrix membranes at the nanoscale: towards structure-performance relationships in CO2/CH4 separation over NH2-MIL-53(Al)@PI, Adv. Funct. Mater. 24 (2014) 249–256.
[28] Y. Li, H.M. Guan, T.S. Chung, S. Kulprathipanja, Effects of novel silane modification of zeolite surface on polymer chain rigidification and partial pore blockage in polyethersulfone (PES)-zeolite a mixed matrix membranes, J. Membr. Sci. 275 (2006) 17–28.
[29] S. Basu, M. Maes, A. Cano-Odena, L. Alaerts, D.E. De Vos, I.F.J. Vankelecom, Solvent resistant nanofiltration (SRNF) membranes based on metal–organic frameworks, J. Membr. Sci. 344 (2009) 190–198.
[30] A.L. Khan, A. Cano-Odena, B. Gutiérrez, C. Minguillón, I.F.J. Vankelecom, Hydrogen separation and purification using polysulfone acrylate-zeolite mixed matrix membranes, J. Membr. Sci. 350 (2010) 340–346.
[31] H. Bux, F. Liang, Y. Li, J. Cravillon, M. Wiebcke, J. Caro, Zeolitic Imidazolate framework membrane with molecular sieving properties by microwave-assisted solvothermal synthesis, J. Am. Chem. Soc. 131 (2009) 16000–16001.
[32] D. Fairen-Jimenez, R. Galvelis, A. Torrisi, A.D. Gellan, M.T. Wharmby, P.A. Wright, C. Mellot-Draznieks, T. Düren, Flexibility and swing effect on the adsorption of energy-related gases on ZIF-8: combined experimental and simulation study, Dalton Trans. 41 (2012) 10752–10762.
[33] M.C. McCarthy, V. Varela-Guerrero, G.V. Barnett, H.K. Jeong, Synthesis of zeolitic imidazolate framework films and membranes with controlled microstructures, Langmuir 26 (2010) 14636–14641.
[34] Y. Pan, Y. Liu, G. Zeng, L. Zhao, Z. Lai, Rapid synthesis of zeolitic imidazolate framework-8 (ZIF-8) nanocrystals in an aqueous system, Chem. Commun. 47 (2011) 2071–2073.
[35] S. Brunauer, P.H. Emmett, E. Teller, Adsorption of gases in multimolecular layers, J. Am. Chem. Soc. 60 (1938) 309–319.
[36] S. Shahid, K. Nijmeijer, High pressure gas separation performance of mixed-matrix polymer membranes containing mesoporous Fe(BTC), J. Membr. Sci. 459 (2014) 33–44.
[37] Z. Chai, X. Zheng, X. Sun, Preparation of polymer microspheres from solutions, J. Polym. Sci. B: Polym. Phys. 41 (2003) 159–165.
[38] M.A. Ray, H. Kim, L. Jia, Dynamic self-assembly of polymer colloids to form linear patterns, Langmuir 21 (2005) 4786–4789.
[39] R.A. Hayes, Amine-modified polyimide membranes, Europen Patent EP 0401005 A1, (1990).
[40] S. Shahid, K. Nijmeijer, Performance and plasticization behavior of polymer-MOF membranes for gas separation at elevated pressures, J. Membr. Sci. 470 (2014) 166–177.
[41] V. Nafisi, M.B. Hägg, Gas separation properties of ZIF-8/6FDA-durene diamine mixed matrix membrane, Sep. Purif. Technol. 128 (2014) 31–38.
[42] A.F. Bushell, M.P. Attfield, C.R. Mason, P.M. Budd, Y. Yampolskii, L. Starannikova, A. Rebrov, F. Bazzarelli, P. Bernardo, J. Carolus Jansen, M. Lanč, K. Friess, V. Shantarovich, V. Gustov, V. Isaeva, Gas permeation parameters of mixed matrix membranes based on the polymer of intrinsic microporosity PIM-1 and the zeolitic imidazolate framework ZIF-8, J. Membr. Sci. 427 (2013) 48–62.
[43] K. Zhang, R.P. Lively, C. Zhang, R.R. Chance, W.J. Koros, D.S. Sholl, S. Nair, Exploring the framework hydrophobicity and flexibility of zif-8: from biofuel recovery to hydrocarbon separations, J. Phys. Chem. Lett. 4 (2013) 3618–3622.
[44] S. Basu, A. Cano-Odena, I.F.J. Vankelecom, MOF-containing mixed-matrix membranes for CO2/CH4 and CO2/N-2 binary gas mixture separations, Sep. Purif. Technol. 81 (2011) 31–40.
[45] T.S. Chung, S.S. Chan, R. Wang, Z.H. Lu, C.B. He, Characterization of permeability and sorption in Matrimid/C-60 mixed matrix membranes, J. Membr. Sci. 211 (2003) 91–99.
[46] D.Q. Vu, W.J. Koros, S.J. Miller, Mixed matrix membranes using carbon molecular sieves–I. Preparation and experimental results, J. Membr. Sci. 211 (2003) 311–334.
[47] Y. Zhang, K.J. Balkus Jr, I.H. Musselman, J.P. Ferraris, Mixed-matrix membranes composed of Matrimid® and mesoporous ZSM-5 nanoparticles, J. Membr. Sci. 325 (2008) 28–39.
[48] L. Zhang, G. Wu, J. Jiang, Adsorption and diffusion of Co_2 and CH_4 in Zeolitic Imidazolate framework-8: effect of structural flexibility, J. Phys. Chem. C 118 (2014) 8788–8794.
[49] C. Sitprasert, F.Y. Wang, V. Rudolph, Z.H. Zhu, Ideal and mixture permeation selectivity of flexible prototypical zeolitic imidazolate framework – 8 membranes, Chem. Eng. Sci. 108 (2014) 23–32.
[50] Q. Yang, C. Zhong, Molecular simulation of carbon dioxide/methane/hydrogen mixture adsorption in metal–organic frameworks, J. Phys. Chem. B 110 (2006) 17776–17783.
[51] T.H. Bae, J.S. Lee, W. Qiu, W.J. Koros, C.W. Jones, S. Nair, A high-performance gas-separation membrane containing submicrometer-sized metal–organic framework crystals, Angewandte Chem.–Int. Ed. 49 (2010) 9863–9866.
[52] A. Huang, W. Dou, J. Caro, Steam-stable zeolitic imidazolate framework ZIF-90 membrane with hydrogen selectivity through covalent functionalization, J. Am. Chem. Soc. 132 (2010) 15562–15564.
[53] T. Yang, Y. Xiao, T.-S. Chung, Poly-/metal-benzimidazole nano-composite membranes for hydrogen purification, Energy Environ. Sci. 4 (2011) 4171–4180.
[54] C. Chmelik, J. van Baten, R. Krishna, Hindering effects in diffusion of CO_2/CH_4 mixtures in ZIF-8 crystals, J. Membr. Sci. 397–398 (2012) 87–91.
[55] J.A. Thompson, J.T. Vaughn, N.A. Brunelli, W.J. Koros, C.W. Jones, S. Nair, Mixed-linker zeolitic imidazolate framework mixed-matrix membranes for aggressive CO_2 separation from natural gas, Microporous Mesoporous Mater. 192 (2014) 43–51.
[56] X.Y. Chen, V.-T. Hoang, D. Rodrigue, S. Kaliaguine, Optimization of continuous phase in amino-functionalized metal–organic framework (MIL-53) based co-polyimide mixed matrix membranes for CO_2/CH_4 separation, RSC Adv. 3 (2013) 24266–24279.
[57] C. Liu, M. Beth, T. W. Stephen, I.B. Annabelle, S. Mark, Metal organic framework-polymer mixed-matrix membranes, (2009), US Patent no. 7637983.
[58] S.N. Wijenayake, N.P. Panapitiya, S.H. Versteeg, C.N. Nguyen, S. Goel, K.J. Balkus, I.H. Musselman, J.P. Ferraris, Surface cross-linking of ZIF-8/polyimide mixed matrix membranes (MMMs) for gas separation, Ind. Eng. Chem. Res. 52 (2013) 6991–7001.
[59] O.G. Nik, X.Y. Chen, S. Kaliaguine, Functionalized metal organic framework-polyimide mixed matrix membranes for CO_2/CH_4 separation, J. Membr. Sci. 413–414 (2012) 48–61.